Research Article
doi: 10.1590/01047760202127012831
vol(27), 2021

CERNE

Oleoresin prospection in *Copaifera* sp. trees by using impulse tomography

Bianca Cerqueira Martins[1iD]✤, Glaycianne Christinne Vieira dos Santos[1iD], João Vicente de Figueiredo Latorraca[1iD]

[1] Federal Rural University of Rio de Janeiro, Seropédica, Rio de Janeiro, Brazil

TECHNOLOGY OF FOREST PRODUCTS

ABSTRACT

Background: Copaiba oil (*Copaifera* L.) is a raw material used by pharmaceutical, cosmetic, and energy industries. However, the difficulty in locating the oleoresin reservoirs, is an obstacle to its continued supply, affecting the sustainable commercialization of the product. So, the potential of impulse tomography for prospecting oleoresin reservoirs in the trunk of 18 *Copaifera* sp. trees was tested, in cross-sections at heights levels 0% (DBH), 25%, 50%, 75%, and 100% (1st fork). The impulse tomography prospections (ITP) were performed only at the 0%, in others 12 trees, because of the risk associated with climbing hollow trees. In total 30 trees were tested. Altogether 102 tomograms were analyzed obtaining: average mechanical wave propagation speed (aMPS), minimum mechanical wave propagation speed (minS) and maximum mechanical wave propagation speed (maxS), prospecting height (Hp%) and total tree height (Ht), diameter at the Hp% (Dhp), and low speed mechanical wave propagation percentage areas (LSa%). These variables were analyzed using multivariate analysis.

Results: The reservoirs were located exclusively at DBH and confirmed by borer prospection increment in 26.7% of the trees. ITP resulted in 37.3% of correct answers and 62.7% of errors, considering the 99 tomograms. However, it was found that the ITP is efficient to indicate sections for which no significant reservoir or hollow presence is expected to be found. The analysis of the main components showed that, except for Ht, the components are good indicators for the location of the reservoirs.

Conclusion: We were able to use tomography to search reservoirs with a significant amount of oleoresin, identify hollow trees, and indicate the exclusion of trees that do not have reservoirs or other alterations.

Keywords: Copaíba, Forest resources, Non-destructive methods, Stress wave, Technology

HIGHLIGHTS

The impulse tomography has the potential to be used for the prospection of oleoresin reservoirs.
Oleoresin reservoirs were identified only at the level of the DBH.
Trees with hollow at early stage may have oleoresin content.
53.3% of the trees of this natural population did not present internal defects in the trunk.

MARTINS, B. C.; SANTOS, G. C. V.; LATORRACA, J. V. F Oleoresin prospection in *Copaifera* sp. trees by using impulse tomography. CERNE, v. 27, e-102831, doi: 10.1590/01047760202127012831

✤Corresponding author e-mail: efbicerq@hotmail.com Received: 08/12/2020 Accepted: 26/07/2021

Open Access
CERNE
ISSN 0104-7760
UFLA UNIVERSIDADE FEDERAL DE LAVRAS

INTRODUCTION

Trees of the *Copaifera* L. genus, classified in the botanical family Leguminosae and Detarioideae subfamily (Azani et al., 2017), have the natural capacity of producing oleoresin, an extractive that is used in various industrial segments for multiple purposes. This substance is composed of resin and essential oils (Pieri et al., 2009). Between 1996 and 2018, 349.7 tons of oleoresin were officially produced in Brazil annually, on average (IBGE, 2020).

According to Rodrigues et al. (2011), oleoresin is produced by secretory glands and accumulates itself in the lumen of secretory channels, distributed along the xylem. These findings were corroborated by Carvalho et al. (2018), Medeiros (2016), Plowden (2003, 2004), and Marcati et al. (2001).

The storage of this content may occur in different parts of the trunk, and there is practical evidence of the occurrence of oil-resiniferous reservoirs ("pockets") that may or may not interconnect (Medeiros, 2016). Ascensão (2007) explained that the plastic deformation of the lumen of the epithelial cells of the secretory channels occurs due to the pressure of the extractive accumulation.

For this reason, probably the presence of large internal areas with oleoresins overflow, hollow and/or fissures represent reservoirs that can be located through technological prospecting.

The study of the internal qualities of trees, such as the presence of hollow sections inside trunks, has been facilitated by the application of methods that employ acoustic wave propagation techniques that can also be used for the evaluation of wood properties, aiming at the improvement of its use (Liu and Li, 2018; Perlin et al., 2015; Arciniegas et al., 2014). To determine the structural integrity of the trees and to evaluate the risk of their fall, or their parts, to prevent accidents, the use of tomography is indicated (ABNT, 2019; Bucur, 2005).

Impulse tomography is based on the propagation of mechanical stress waves generated from hammer shocks (Mendes and Silva Filho, 2019; Carrasco et al., 2017; Castro et al., 2011). The emission and capture of signals, which result in time and distance information, with which propagation speed is calculated, is done by sensors attached to the trunk by metal nails (Heidelberg, 2011).

Wood quality and its intraspecific variability can be studied to understand the mechanisms of trees development, in terms of structure, shape, and biological functioning (Arciniegas et al., 2014). The results of several acoustic tomography studies have already demonstrated that the graphic representations (tomographic images) and wave paths obtained from cross-sections of the tree trunk are largely correlated with the internal condition of deterioration or existing defects (Xiaochen et al., 2018; Secco et al., 2012; Pereira et al., 2007).

Other studies validated the use of tomography to determine the physical properties of wood, such as resistographic amplitude (Rollo et al., 2013), moisture content (Putri et al., 2017); Latorraca et al., 2011), and mechanical properties (Young and shear modulus) (Gonçalves et al., 2014; Gonçalves et al., 2011; Sedik et al., 2010), elasticity modulus (Carrasco et al., 2017), knots interference, juvenile wood, and reaction wood (Palma et al., 2018). Also, research was carried out to determine the pith´s location (Perlin et al., 2018) and address aspects related to wood anisotropy (Perlin et al., 2019; Arciniegas et al., 2014).

Considering the technological potential of this inspection technique, this study aimed at prospecting oleoresin reservoirs in the stem of native *Copaifera* trees through impulse tomography.

MATERIAL AND METHODS

Characterization of the site

The site under study is in western Amazon, in the state of Acre - Brazil (Figure 1). The climate in this region is characterized as equatorial, with three well-defined seasons: drought (June–August), rainy (October–April), and a transition period in May and September (Duarte, 2017). The soils are dystrophic, deep, and well-drained, classified as Oxisols. In general, the landscape presents a flat to gently undulating relief and the prevailing vegetation cover are Open Forest with Bamboo, Open Forest with Palm and Dense Forests (ACRE, 2010), besides anthropized areas.

Data acquisition

The impulse tomography prospections (ITP) were conducted in September 2018 and July 2019. The used procedures followed the recommendation by Heidelberg (2011) and the adaptations of Castro (2011) and Perlin et al. (2015) methods. Thirty trees were evaluated using the Arbotom® mechanical pulse tomograph, with eight sensors. According to Arciniegas et al. (2014), at least six sensors are required to detect internal defects.

ITP was performed longitudinally across the trunk of 18 trees, in cross-sections, at five prospection height levels (Hp%), from DBH (1.30 m from the ground surface or diameter at breast height), 100% (first stem bifurcation) and 25%, 50%, 75%, determined form the DBH. For this, climbing and rappelling equipment was used, and two climbers collaborated. In 12 other trees, the ITP was performed at DBH, due to the risk associated with climbing hollow trees, the existence of physical impediments (vines, swarms, and others), or the difficulty to install the climbing equipment.

The configuration used in Arbotom® tomograph for the reconstruction of the images consisted of a) velocity filter: 50 to 4000 m/s; b) color model: purple-red-yellow-green; c) 2D resolution = 5 mm; d) selection of the faster mean value and distribution analysis; e) correction of standard deviation and maximum standard deviation = 1; f) diffuse porosity. Each tomogram has been configured according to its mechanical wave propagation speed (MPS) scale. For the validation of the prospection, samples were extracted from the wood using a Pressler auger, in the radial direction, taken according to the interpretation of the tomograms, immediately after performing the ITP. When the reservoirs were located, oleoresin samples were collected, for 15 minutes, in the same drilling done by the Pressler auger. Areas of interest were those that, in the scale (MPS vs. colors), presented pink, red, and orange pigmentation because they were associated to low speeds, in contrast to yellow and green, associated to highest speeds.

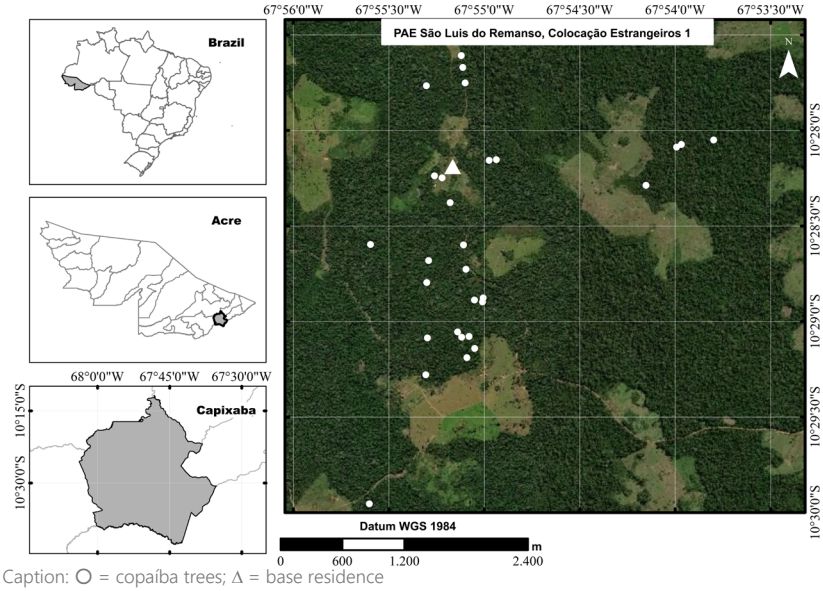

Caption: ○ = copaíba trees; Δ = base residence

Fig. 1 Population site of *Copaifera* sp. prospected using impulse tomography.

Data analysis

We analyzed 102 tomograms obtained through an inversion algorithm that generates line graphs and 2D graphs, based on 56 mechanical wave paths. Tomograms that showed inconsistent readings, related to percentage prospecting height level (Hp%) 75% and 100% from tree 9 and (Hp%) 0% from tree 10, were excluded. Therefore, statistical analysis was performed using information from 99 tomograms.

The percentage of hits and misses of tomography impulse were verified, adopting three conditions as the categorization criteria (Table 1). The categories identified for the internal condition of the cross-sections of the trunks of *Copaifera* were defined from the condition indicated on the tomography before drilling, from the condition verified through the translation and through the type of characteristic identified (hollow or reservoir). The evaluation by criteria was adopted in the segmentation of the different characteristics of the stem of the trees, aiming to identify the characteristic of interest of the study (reservoir correctly identified by tomography (P-PR) and by probing) of the other conditions found.

The percentage of areas with low-speed propagation of mechanical wave (LSa%) was quantified, grouping the trees according to the following classes: a) LSa% ≤ 20% = low; b) 20% < LSa% ≤ 30% = average; c) 30% < LSa% ≤ 50% = high; d) LSa% > 50% = very high. The classes adopted were established, adapting the classification proposed by Rollo (2013). The Arcmap 10.6.1 software (ESRI, 2018), was used to measure LSa%.

Tab. 1 Categorization criteria for the condition of the cross-sections of the trunks of *Copaifera* sp.

Category	Condition			
	Before	After	Feature	
			Hollow	Reservoir
P-PH	1	1	1	0
P-PR	1	1	0	1
P-PHR	1	1	1	1
P-AHR	1	0	1	1
A-AHR	0	0	1	1
A-PHR	0	1	1	1

Caption: 1 = presence; 0 = absence; Before = before prospecting drilling; After = after prospecting drilling; Hollow = hollow in the trunk; Reservoir = oleoresin reservoir; P = presence of hollow or reservoir; A = absence of hollow or reservoir. Each letter of the category corresponds to one of the conditions presented in the table, for example: P-PH = Presence of hollow before and after prospecting drilling.

The variables were tested for multivariate normality distribution, Pearson's correlation, and Principal Component Analysis (PCA). The variables data were centered at zero and rescaled to unit variance. For the PCA, Ferreira (2018) and Valentin (2012) guidelines were followed. The data mining was performed in the Paleontological Statistics - Past 4.02 software (Hammer et al., 2001).

Regarding the components of interest for ITP, the variables MPS = mechanical wave propagation speed (m/s); aMPS = average; Ht = total tree height (m); Hp% = prospecting heights (%); minS = minimum mechanical wave propagation speed (m/s); maxS = maximum mechanical wave propagation speed (m/s); Dhp = diameter in Hp% (cm); LSa% = percentage of area with low speeds of mechanical wave propagation (%) were considered, and organized in a 7 x 99 dimension matrix (variables x observations).

The longitudinal tomographic profiles of the prospected trees, which had reservoirs, were elaborated using Adobe Photoshop software, version 20.0.0.

RESULTS

Considering the five-prospection height levels and the 56 wave paths, which constitute each tomogram, the statistic amplitude of the MPS was 3130 m/s, the minimum MPS 106 m/s, and the maximum MPS was 3236 m/s.

The dendrometric aMPS and LSa% characteristics of the studied trees are available in Table 2. The LSa% analysis from the DBH tomograms section showed that 50% of the trees have less than 20% of the area affected by low speed and belong to the low LSa% category, 7% to the medium LSa%, 30% to the high LSa%, and 13 % to the very high LSa%. At DBH, aMPS varied between 304 m/s and 1123 m/s, their respective standard deviation (Sd) and coefficient of

variation (CV) showed high values. It was found that the linear correlation between DBH and Ht is negligible (R = 0.37, R^2 = 0.14, p = 0.045) as well as Dhp and Hp% (R = -0. 3751, R^2 = 0.1589, p = 0.00012).

ITP resulted in 37.3% of correct answers and 62.7% of errors, considering the 99 tomograms. The errors represent the percentage of tomograms that seemed to mistakenly indicate the existence of reservoirs, hollows, or internal fissures. Therefore, they were classified in the P-AHR category. The correct answers were distributed as follows: P-PH (3.0%), P-PR (8.1%), P-PHR (3.0%), and A-AHR (23.2%). Associating the results of the A-AHR and A-PHR (0%) criteria, it was found that ITP is efficient in the function of discarding sections where there is no significant reservoir or the presence of hollow. The A-AHR category considered the possibility that the tomogram would indicate the absence of a cavity or reservoir. Later, this condition would be confirmed by the auger. In addition, there was also no category A-PHR, which admitted the possibility that the tomogram showed the absence of a cavity or reservoir and the auger showed the presence of these conditions.

Table 3 presents the PCA summary, where the primary axes (PC1, PC2, and PC3) explain 68.63% of the variation between the seven components combined in this study. PC1 shows the relationship between maxS., aMPS, minS and the main component of greater explanation (27.87%).

It is observed that the tomograms of the cross-sections that presented an oleoresin reservoir were grouped in the characteristic quadrants by low aMPS (Figure 2). In the PC2 axis, the strong and positive charges highlighted Dhp and LSa%, and the negative charges highlighted the Hp%. The sections with the absence of reservoirs can be observed in the entire trunk but rarely when there is a predominance of lower aMPS. In PC3, the latent variables Ht and LSa% complement the set of variables that explain the variance ordering structure. Despite the important role of LSa% confirmed in the PCA, there was a great variation (4.73% - 65.7%) of this parameter in the trees with reservoirs.

Tab. 2 Dendrometric and mechanical wave propagation speed parameters in the DBH of trunks of copaíba trees (*Copaifera* sp.), transversal plane.

Tree	DBH (cm)	Ht (m)	Speed across (m/s)					LSa %
			aMPS	Sd (±)	CV (%)	minS	maxS	
A01	90.72	19.40	482	333	69.02	198	1586	30.4
A03	52.52	23.00	412	309	29.92	106	819	13.6
A08	153.43	31.50	804	342	51.55	406	1728	33.0
A09	34.70	20.80	403	248	24.24	218	743	7.0
A11	53.16	23.37	429	189	23.24	172	673	19.2
A17	104.41	32.00	939	137	29.73	455	1722	15.3
A18	70.03	27.00	1123	290	33.46	443	2012	1.4
A19	71.62	26.00	764	388	50.78	262	1995	0.0
A20	64.62	29.30	622	322	40.49	216	1457	30.4
A21	52.84	26.50	939	333	39.64	336	1755	0.0
A22	86.58	31.00	871	342	41.10	337	1646	0.0
A23	53.16	23.38	820	279	37.37	381	1554	7.6
A25	77.35	21.55	599	407	56.83	406	1728	33.3
A27	92.63	30.00	534	372	54.31	220	1030	76.7
A28	109.18	27.00	785	358	55.38	266	1492	50.6
A29	92.31	31.00	758	307	42.47	233	2114	31.1
A04^{r}	64.30	33.80	492	165	62.92	145	1504	27.4
A05^{r}	79.58	27.00	439	98	37.54	171	817	4.73
A13^{r}	66.21	20.30	451	188	44.93	263	1280	60.6
A14^{r}	74.80	30.38	501	209	49.57	166	1547	65.7
A02^{h}	43.93	28.00	508	123	72.73	164	1662	46.2
A06^{h}	120.96	26.00	356	100	53.25	114	693	14.7
*A10^{h}	29.92	19.50	-	-	-	-	-	-
A16^{h}	145.79	33.00	484	189	33.33	302	1141	30.4
A15^{h}	143.88	32.00	389	161	53.67	166	935	2.4
A26^{h}	113.32	35.00	423	252	32.31	293	1600	23.3
A07h^{r}	178.89	22.00	304	90	94.52	257	1030	32.0
A12h^{r}	112.37	23.15	371	287	24.31	177	607	32.9
A24h^{r}	110.14	30.00	530	376	35.72	260	973	11.9
A30h^{r}	149.61	30.00	620	340	53.80	298	1589	13.9

Caption: * The tree tomogram was excluded; Ht = total tree height (m); DBH = diameter at breast height (cm); aMPs = average mechanical wave propagation speed (m/s); Sd= standard deviation; CV = coefficient of variation. minS = minimum MPS (m/s); maxS = maximum MPS (m/s); LSa% = percentage of area with low speeds of mechanical wave propagation (%); r = reservoir; hr = hollow and reservoir; h = hollow.

Tab. 3 Proportion of the total variance explained by the compensations between components of interest from the ITP, eigenvalues (λ), and loads in explanatory percentages (%) of the PCA axes.

PCA Summary				Loadings						
PC	λ	%	% accumulated	aMPS	Ht	Hp%	Dhp	minS	maxS	LSa%
1	1.95	27.87	27.87	0.54	0.04	-0.08	0.25	0.41	0.64	0.26
2	1.66	23.77	51.64	-0.31	0.17	-0.53	0.59	-0.18	-0.11	0.45
3	1.19	16.99	68.63	0.37	0.69	-0.16	0.13	-0.33	-0.02	-0.49
4	0.82	11.78	80.41	-0.23	0.63	0.60	-0.03	0.18	-0.03	0.40
5	0.73	10.45	90.86	0.10	-0.22	0.39	0.14	-0.79	0.34	0.19
6	0.48	6.92	97.78	-0.01	-0.21	0.42	0.74	0.21	-0.21	-0.37
7	0.15	2.22	100.00	0.65	-0.09	0.05	-0.02	-0.05	-0.64	0.40

Caption: aMPs = average mechanical wave propagation speed (m/s); Ht = total tree height (m); Hp% = prospecting heights (%); Dhp = diameter in Hp% (cm); minS = MPS minimum (m/s); maxS = MPS maximum (m/s); LSa% = percentage of area with low speeds of mechanical wave propagation (%).

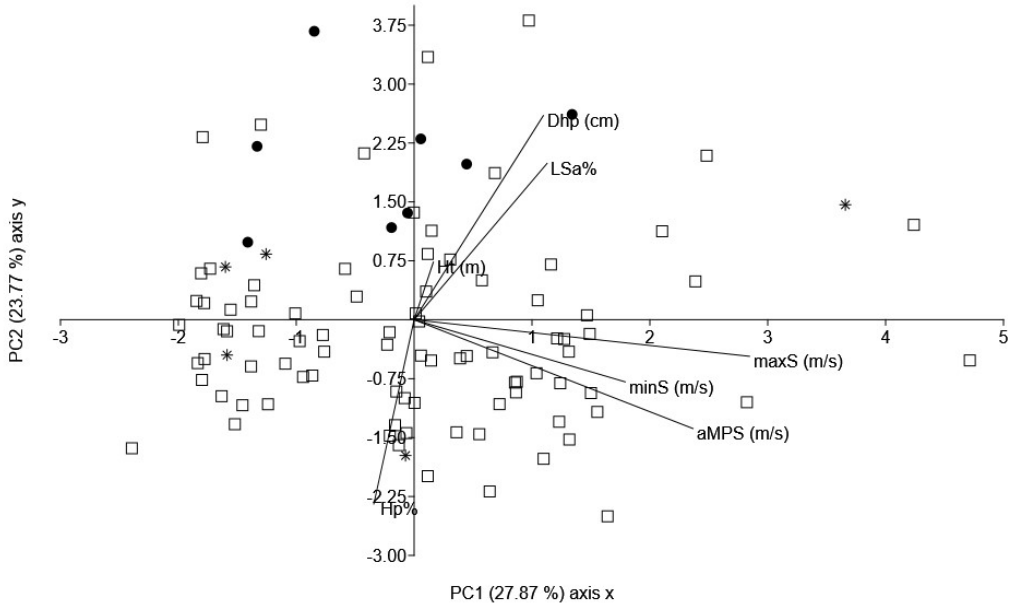

Fig. 2 Biplot analysis of main components (PC1 and PC2) and grouping by tomograms of the cross-sections of Copaifera sp. trees similarities. Caption: Sections with oleoresin reservoirs are represented ●; sections with oleoresin *; and sections without oleoresin ☐.

Among 99 tomograms analyzed, eight were had reservoirs (8.1%), of which four (4%) coincided with hollow regions. Another two (2%) contained fissures, and eighty nine (89.9%) did not present any of these conditions in the position verified by the Pressler auger.

Taking into consideration only the height of the DBH of the 30 trees, the oleoresin reservoirs were located in eight (26.7%), allowing to obtain expressive volumes of oleoresin (A04 = 3600 ml, A05 = 50 ml, A12 = 40 ml, A13 = 1600 ml, A14 = 2300 ml, A24 = 50 ml and A07 and A30 <20 ml). Altogether, ten trees were hollow (20%), but four (13.3%) were identified as hollow trees with oleoresin reservoirs. These reservoirs were not found in other Hp% of the trunks. Thus, 53.3% of the tree did not present internous discontinuities.

The sampling effort used (five heights levels) and the results obtained do not allow us to state that there are no "pockets" of oleoresin at different heights from DBH. Even fissures at a height of 25% and, in some cases, regions with oleoresin odor were identified. Also, it was possible to monitor and verify that, at 25%, 50%, and 100% heights, 34% of the trees drained or continued to drain oleoresin after 19 months, since the first prospection, despite the pin used to interrupt the drilling holes of the perforations.

The tomogram of transversal sections along the trunk of the trees, with potential main oleoresin reservoirs are shown in Figure 3.

DISCUSSION

The percentage of errors and success obtained indicate that the occurrence of low MPS (pink, red, and orange colors) is a good criterion to choose the appropriate trunk drilling location and oleoresin extraction.

However, it is important to note that, on a tomogram, the colors did not exactly correspond to the size of the internal anomaly or its exact location. The portions are

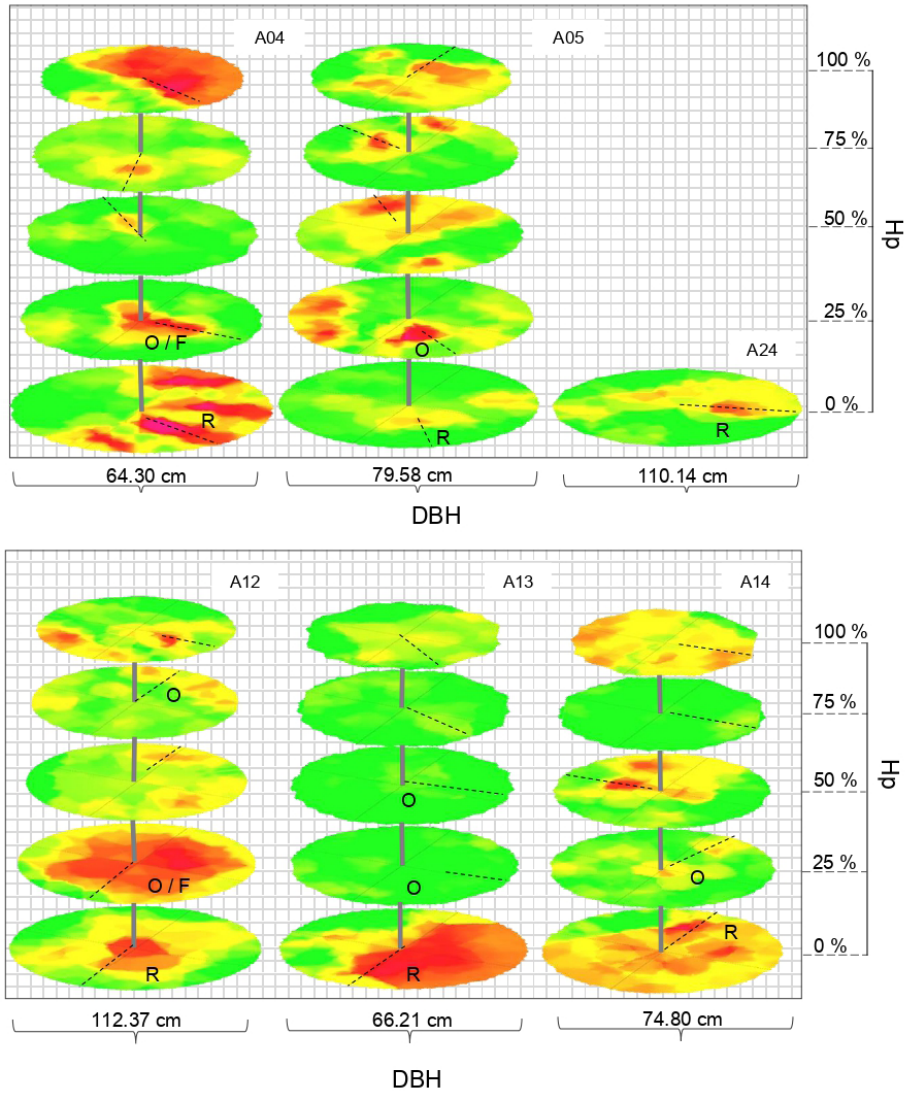

Fig. 3 Tomogram of transversal sections along the trunk of *Copaifera* sp. trees, in which oleoresin reservoirs were identified. Caption: a) diameter at breast height level (DBH); b) percentual height level of prospection (Hp%); ---- = radial core removal direction (RRD); O = Hp% with indication of oleoresin occurrence; F = Hp% with fissure; R = oleoresin reservoirs occurrence in the DBH, in the region indicated by the RRD.

represented by high speeds (in this case, yellow and green colors) consistently illustrated mechanically cooperating portions (Heidelberg, 2004). Moreover, as can be seen in Figure 3 (A05), even areas of orange-yellow colors may represent a reservoir, and areas characteristically orange or red do not necessarily represent a reservoir or hollow.

The performance of additional physical studies may contribute to the reduction of the percentage of errors (62.7%), considering that it is possible that there are cracks, or even initial reservoirs, in displaced positions, that a single probe was not able to access. This research proposed a method of verifying the potential of impulse tomography (a survey by Hp%), seeking to minimize the impact on the individuals studied, due to the fact that they are native trees and constitute a population distributed over a wide geographical space, that is, of great ecological importance.

Those with predominantly low MPS, but not confirmed as reservoir indicators, can be explained by understanding different factors. For example, mechanical wave propagation is strongly influenced by the mechanical properties, density, and modulus of elasticity wood (Schimleck et al., 2019; Vidaurre et al., 2013).

This effect could also be explained by the variation of the moisture content (MC%) of the wood at the time of the tomography (Bucur, 2005). Latorraca et al. (2011) checking the relationship between moisture content (MC%) of wood and MPS from *Pinus caribaea*, concluded that moisture influences the formation of the tomographic image and that higher MC% results in lower MPS. Longitudinally, the authors observed that the humidity in the higher zone discs was higher than in the lower zone discs. This behavior was not observed in copaiba trees in our study.

Another important factor is the wood density variation. Alves et al. (2013, p.12) concluded that "the increase in density provides a higher value of MPS in the normal direction of the fibers", but "density is not the only

parameter to affect speed". But, high density woods with a lot of discontinuities do not have high velocity of wave propagation. For Bucur (2006), this issue a little more complex, because she observed that can be an increase in velocity with the increase in density, as well as a reduction in velocity with the increase in density, and there can be independence between these two factors. Fathi et al. (2020), used guided wave propagation and artificial neural network to predict the mechanical properties of wood, and stated that wave velocity is highly sensitive to the moisture content, density, and mechanical properties of wood.

The mechanical wave propagation is strongly influenced by mechanical properties, density, and modulus of elasticity. In this sense, it is important to consider the arguments of Vidaurre et al. (2013) regarding the influence of tension wood formation on wood properties in trees. Tension wood can occur in tropical trees that are not inclined, when the spacing is denser, due the movement of the canopy to obtain light (Timell, 1986; Warenjö, 2003 Apud Vidaurre et al., 2013, p. 27). Mendes and Silva Filho (2019) found that impulse tomography was efficient in identifying zones with different densities, related to tension wood.

Vidaurre et al. (2013) found that the modulus of elasticity (MoE) in medium flexion, a mechanical property of tension wood, was higher at all humidity levels, compared to normal wood, due to the gelatinous layer present in the secondary fibers wall, although its effect on the basic density is not significant, because the tension wood has no significant influence on the cell wall proportion (Vidaurre et al., 2013).

The tropical forest species, with defects and structural irregularities, besides their specific mass, will have a variable modulus of elasticity (Moreschi, 2012). Mechanical wave propagation speed is influenced by MoE and density. MoE is influenced by the species, moisture content, width of the growth rings, position of removal of piece along the tree stem, percentage initial and latewood and differentiation between juvenile and adult wood, as well as external influences (Cunha and Mattos, 2010).

Also, in the context of the formation of the tension wood, the location of the pith, influenced by the eccentricity of the stem (displacement of the pith out of the center), affects the result of the stem of trees quality evaluation, because it has a great influence on the wood anisotropy.

It is necessary to consider that anisotropy plays a major role in the construction of tomographic images. According to Perlin et al. (2015), anisotropy and hygroscopic behavior of wood should be considered when using tomography to locate internal heterogeneity.

It is argued that the location of the pockets, exclusively in the region of the DBH, may originate from phenomena that trigger the formation of hollows since they were not found in the higher levels Hp%. For Spatz and Niklas (2013), the formation of cavities in cross-sections, in some cases, can be understood as a natural strategy of evolutionary "engineering" that enables several plants to grow vertically without bending under their weight.

It is also necessary to evaluate the mechanical impact caused by forest mastofauna. Some animals have the habit of looking for the *Copaifera* trees in search of its fruits and oil itself when they are not fructifying (Shanley and Medina, 2005). This process can cause injuries to the stem, which is a gateway for xylophagous agents.

In research carried out in Indonesia, Putri et al., (2017) evaluated, through sonic tomography, the formation of resin in the wood of *Aquilaria malaccensis* Lam, verifying that areas damaged by the *Fusarium solani* fungus indicate the formation of resinous wood.

It cannot be ruled out, however, that both the positioning and the injuries size influence the probability of detecting deteriorated regions by using a tomographic image (Espinosa et al., 2020), and that prospecting with the Pressler auger may not have accessed the exact region of reservoirs location or deformations.

The reservoirs occurred in trees with DBH > 60 cm, coinciding with what was concluded by Martins et al. (2008), who found a possible non-linear relationship between DBH and oleoresin production. According to Martins et al. (2016) there is great individual morphological and physiological variation in *Copaifera* trees, which leads to a lack of definition regarding the establishment of a DBH in which there is a guarantee of obtaining oleoresin. The authors cite reports of productive trees with DBH> 35 cm.

A weak negative linear correlation was found between diameters and heights, which is an expected result. Roquette et al. (2018) attributed a similar result to the heterogeneity of the trees and the factors that affect growth. In practice, the diameter of the copaíbas slowly decreases as the height increases, giving the stem of *Copaifera* trees a cylindrical shape.

To achieve greater precision, it is necessary to understand more deeply different physical-mechanical, anatomical, and chemical parameters of the woody tissue of the *Copaifera*, as well as the environmental and ecological aspects and their interactions. According to Schimleck et al. (2019), advancement in non-destructive evaluation techniques will improve the understanding of the impact of wood properties on product performance.

CONCLUSIONS

Impulse tomography can safely indicate hollow trees and the exclusion of trees that do not have oleoresin reservoirs.

It can guide the prospecting of reservoirs with a capacity to supply a significant amount of oleoresin, even in hollow trees.

The correct answers of the ITP (37.3%) were obtained, mainly, at the time of the DAP, where the existence of the reservoirs was verified. The 62.7% of errors verified with the drilling occurred in the upper parts of the trunks where there was no identification of an oleoresin reservoir, such results indicate that further physical studies of *Copaifera* wood are necessary for a future improvement of the technique.

The low aMPS standard and LSa% are important indicators for determining the location of oleoresin reservoirs, but they should not be the only criteria for making decisions about trunk drilling.

It is recommended to perform the prospection with impulse tomography at the height of the DBH of the trees, due to the non-detection of significant reservoirs in higher Hp.

ACKNOWLEDGMENTS

Acre Federal University (UFAC), Coordination for the Improvement of Higher Education Personnel (CAPES), Wood Quality and Anatomy Research Center (NPQM).

REFERENCES

ABNT NBR 16246-3: Florestas urbanas – Manejo de árvores, arbustos e outras plantas lenhosas. Parte 3: Avaliação de risco de árvores. 2019. 14p.

ACRE - Governo do Estado do Acre. Zoneamento Ecológico-Econômico do Estado do Acre, Fase II (Escala 1:250.000): Documento Síntese. Rio Branco: Secretaria Estadual de Meio Ambiente (SEMA), 2010. 356p.

ALVES, R. C.; MARTINS, T.; CARRASCO, E. V. M. Influência da densidade na velocidade de propagação da onda em sete espécies de madeira tropicais. Natural Resources, v.3, n.1, p. 6-13, 2013.

ARCINIEGAS, A.; PRIETO, F.; BRANCHERIAU, L. C.; LASAYGUES, P. Literature review of acoustic and ultrasonic tomography in standing trees. Trees, n.28, p.1559-1567, 2014.

ASCENSÃO, L. Estruturas secretoras em plantas. Uma abordagem morfo-anatómica. In: FIGUEIREDO, A. C; BARROSO, J. G; PEDRO, L. G. Potencialidades e Aplicações das Plantas Aromáticas e Medicinais. Faculdade de Ciências da Universidade de Lisboa, Lisboa, Portugal, n.3, p.19-28, 2007.

AZANI, N.; BABINEAU, M.; BAILEY, C. D.; BANKS, H.; BARBOSA, A. R.; PINTO, R. B. A new subfamily classification of the Leguminosae based on a taxonomically comprehensive phylogeny. TAXON, v.66, n.1, p. 44–77, 2017.

BUCUR, V. Ultrassonic tecniques for nondestrutive testing of standing trees. Ultrasonics. v.43, n.4, p.237-239, 2005.

BUCUR, V. Acoustics of wood. Springer. 2006. 399p.

CARRASCO, E. V. M.; SOUZA, M. F.; PEREIRA, L. R. S.; VARGAS, C. B.; ANTILLA, J. N. R. Determinação do módulo de elasticidade da madeira em função da inclinação das fibras utilizando tomógrafo acústico. Matéria, v.22, n.1, 2017.

CARVALHO, D. C.; PEREIRA, M. G. G. P.; LATORRACA, J. V. F.; PACE, J. H. C.; SILVA, L. D. S. A. B.; CARMO, J. F. Dendrochronology and growth of *Copaifera langsdorffii* wood in the vegetative dynamics of the Pirapitinga Ecological Estation, state of Minas Gerais, Brazil. Floresta, v.48, n.1, p.49-58, 2018.

CASTRO, V. R.; FILHO, M. T.; ARIZAPANA, M. A.; SILVA, J. C.; SILVA FILHO, D. F.; POLIZEL, J.; BELINI, U. Avaliação do perfil radial do lenho de árvores de teca (*Tectona grandis* L.f.) através da Tomografia de Impulso. Floresta e Ambiente, v.18, n.2, p.144-152, 2011.

CUNHA, A. B.; MATOS, J. L. M. Determinação do módulo de elasticidade em madeira laminada colada por meio de ensaio não destrutivo ("stress wave timer"). Rev. Árvore, v.34, n.2, p.345-354, 2010.

DUARTE, A. F. Climatologia das chuvas e efeitos antrópicos da urbanização na bacia do Rio Acre, Amazônia Ocidental. Boletim do Observatório Ambiental Alberto Ribeiro Lamego. v.11, n.1, p.199-213, 2017.

ESPINOSA, L.; PRIETO, F.; BRANCHERIAU, L.; LASAYGUES, P. Quantitative parametric imaging by ultrasound computed tomography of trees under anisotropic conditions: Numerical case study. Ultrasonics. v.102, 2020.

ESRI, 2018. ArcGIS Desktop. Redlands, CA.

FATHI, H.; NASIR, V.; KAZEMIRAD, S. Prediction of the mechanical properties of wood using guided wave propagation and machine learning. Construction and Building Materials, v.262, n.120848, 2020.

FERREIRA, D. F. Estatística Multivariada. UFLA, 2018. 624p.

GONÇALVES, R.; TRINCA, A. J.; CERRI, D. G. Comparison of elastic constants of wood determined by ultrasonic wave propagation and static compression test. Wood and Fiber Science, v.43, n.1, p. 64-75, 2011.

GONÇALVES, R.; TRINCA, A. J.; PELLIS, B. P. Elastic constants of wood determined by ultrasound using three geometries of specimens. Wood Science and Technology, v.48, p. 269–287, 2014.

HAMMER Ø; HARPER, D. A. T.; RYAN, P. D. PAST: Paleontological Statistics. Software Package for Education and Data Analysis. Palaeontologia Electronica, v.4, n.1, 2001.

HEIDELBERG, F. R. Statische Hinweise im Schall-Tomogramm von Bäumen. Stadt und Grün. v.7, p. 41-45, 2004.

HEIDELBERG, F. R. User Manual: Arbotom® 3D Tree Impulse Tomograph. Rinntech, v. 17, n.2. p. 124-128, 2011.

IBGE - Instituto Brasileiro de Geografia e Estatística. Produção da extração vegetal e da silvicultura - Tabela 289: Quantidade produzida e valor da produção na extração vegetal, por tipo de produto extrativo: copaíba (óleo), 2020. Sistema IBGE de recuperação automática – SIDRA. Available at: https://sidra.ibge.gov.br/tabela/289#notas-tabela. Accessed in: July 24th 2020.

LATORRACA, J. V. F.; RODRIGUES, N. D.; VIEIRA, M. C.; OHANA, C. C.; TEIXEIRA, J. G. Efeito da umidade da madeira na propagação de ondas mecânicas. Floresta e Ambiente, v.18, n.4, p. 451-459, 2011.

LIU, L.; LI, G. Acoustic tomography based on hybrid wave propagation model for tree decay detection. Computers and Electronics in Agriculture**,** n.151, p. 276–285, 2018.

MARCATI, C. R.; ANGYALOSSY-ALFONSO, V.; BENETATI, L. Anatomia comparada do lenho de *Copaifera langsdorffii* Desf. (Leguminosae-Caesalpinoideae) de floresta e cerradão. Brazilian Journal of Botany, v.24, n.3, p. 311-320, 2001.

MARTINS, K.; SILVA, M. G. C.; RUIZ, R. C.; ARAÚJO, E. A.; WADT, L. H. O. Produção de oleorresina de copaíba (*Copaifera* spp.) no Acre. In: Editora WADT, L. H. O., Anais do Seminário Manejo de Produtos Florestais não-Madeireiros na Amazônia, Rio Branco: Embrapa Acre, v1, p. 100-107, 2008. Available at: https://www.alice.cnptia.embrapa.br/alice/bitstream/doc/505903/1/kamukaia.pdf. Accessed in: November 27th 2020.

MARTINS, K.; AZEVEDO, C. R.; SILVA, M. G. C.; OLIVEIRA, W. L. H. Copaíba: aspectos ecológicos e potencial de uso do oleorresina. In: SIVIERO, A.; MING, L. C.; SILVEIRA, M.; DALY, D.; WALLACE, R. Etnobotânica e Botânica Econômica do Acre. Edufac, 2016. 410p.

MEDEIROS, R. S. Estudo da anatomia do lenho e dendrocronologia de árvores de *Copaifera multijuga* Hayne na Amazônia brasileira e sua relação com o manejo e extração de oleorresina. 2016. 190 p. PhD thesis Universidade de São Paulo, Piracicaba.

MENDES, F. H.; SILVA FILHO, D. F. Frequency variation of mechanical waves of the impulse tomograph based on geographic north. Sci. For. v.47, n.122, p. 353-358, 2019.

MORESCHI, J. C. Propriedades da Madeira. Departamento de Engenharia e Tecnologia Florestal – UFPR. Paraná, 2012. v.4, p. 01-208, 2012.

PALMA, S.; GONÇALVES, R.; TRINCA, A.; COSTA, C.; REIS, M.; MARTINS, G. Interference from knots, wave propagation direction, and effect of juvenile and reaction wood on velocities in ultrasound tomography. BioRes, v.13, n.2, p. 2834-2845, 2018.

PEREIRA, L. C.; SILVA FILHO, D. F.; TOMAZELLO FILHO, M.; COUTO, H. T. Z.; MOREIRA, J. M. M. A.; POLIZEL, J. L. Tomografia de impulso para avaliação do interior do lenho de árvores. Revista da Sociedade Brasileira de Arborização Urbana, v.2, n.2, p. 65-75, 2007.

PERLIN, L. P.; JULIANI, M. A.; VALLE, A.; PINTO, R. C. A. Mathematical basis of ultrasonic tomography for integrity evaluation of wood structural elements. Cerne, v.21, n.3, p. 503-509, 2015.

PERLIN, L. P.; PINTO, R. C. A.; VALLE, A. Ultrasonic tomography in wood with anisotropy consideration. Construction and Building Materials, v.229, n.116958, 2019.

PERLIN, L. P.; VALLE, A.; PINTO, R. C. A. New method to locate the pith position in a wood cross-section based on ultrasonic measurements. Construction and Building Materials, v.169, p. 733-739, 2018.

PIERI, F. A.; MUSSI, M. C.; MOREIRA, M. A. S. Óleo de copaíba (*Copaifera* sp.): histórico, extração, aplicações industriais e propriedades medicinais. Rev. bras. plantas med., v.11, n.4, p. 465-472, 2009.

PLOWDEN, C. Production ecology of Copaíba (*Copaifera* spp.) oleoresin in the eastern Brazilian Amazon, Economic Botany. v.57, p. 491–501, 2003.

PLOWDEN, C. Copaíba (*Copaifera* spp.). In: SHANLEY, P.; PIERCE, A. R.; LAIRD, S. A.; GUILLEN, A. Explotando el Mercado verde: certificación y manejo de productos forestales no maderables. Manuales de conservación de la serie pueblos y plantas. WWF, UNESCO, Royal Botanic Gardens: Nordan-Comunidad. 2004, 447p.

PUTRI, N.; KARLINASARI, L.; TURJAMAN, M.; WAHYUDI, I.; NANDIKA, D. Evaluation of incense-resinous wood formation in agarwood (*Aquilaria malaccensis* Lam.) using sonic tomography. Agriculture and Natural Resources, v.51, n.2, p.84-90, 2017.

RODRIGUES, T. M.; TEIXEIRA, S. P.; MACHADO, S. R. The oleoresin secretory system in seedlings and adult plants of copaíba (*Copaifera langsdorffii* Desf., Leguminosae–Caesalpinioideae). Flora-Morphology, Distribution, Functional Ecology of Plants, v.206, n.6, p. 585–594, 2011.

ROLLO, F. M. A; SOAVE JUNIOR, M. A.; VIANA S. M.; ROLLO, L. C. P.; COUTO, H. T. Z.; SILVA FILHO, D. F. Comparison between resistography readings and tomographic images for internal assessment in tree trunks. Cerne, v.19, n.2, p. 331-337, 2013.

ROQUETTE, J. G.; DRESCHER, R.; BRONDANI, G. E.; RONDON NETO, R. M.; EBERT, A.; TEIXEIRA, L. R.; DIAS, A. P.; GAVA, F. H. Age and growth affect oleoresin yield from copaiba trees in the Cerrado–Amazônia ecotone. Cerne, v. 24, n. 2, p. 106-113, 2018.

SCHIMLECK, L.; DAHLEN, J.; APIOLAZA, L. A.; DOWNES, G.; EMMS, G.; EVANS, R., MOORE, J.; PÂQUES, L.; VAN DEN BULCKE, J.; WANG, X. Non-destructive evaluation techniques and what they tell us about wood property variation. Forests, v.10, n.728, 2019.

SECCO, C. B.; GONÇALVES, R.; CERRI, D. G.; VASQUES, E. C.; BATISTA, F. Behavior of ultrasonic wave propagation in the presence of holes. Cerne, v.18, n.3, p. 507-514, 2012.

SEDIK, Y.; HAMDAN, S.; JUSOH, I.; HASAN, M. Acoustic properties of selected tropical wood species. Journal of Nondestructive Evaluation, v.29, p. 38-42, 2010.

SHANLEY, P.; MEDINA, G. Frutíferas e plantas úteis na vida Amazônia. In: CYMERYS, M.; FERNANDES, N. M. P.; RIGAMONTE-AZEVEDO, O. C. Copaíba: *Copaifera* L. f. CIFOR, Imazon, 2005. p.183-187.

SPATZ, H. C.; NIKLAS, K. J. Modes of failure in tubular plant organs. American Journal of Botany, v.100, n.2, p.332–336, 2013.

VALENTIN, J. L. Ecologia Numérica: Uma introdução à análise multivariada de dados ecológicos. Editora Interciência, 2012. 168p.

VIDAURRE, G. B.; LOMBARDI, L. R.; NUTTO, L.; FRANÇA, F. J. N.; NISTAL, F. J.; OLIVEIRA, J. T. S.; ARANTES, M. D. C. Propriedades da madeira de reação. Floresta e Ambiente, v.20, n.1, p. 26-37, 2013.

XIAOCHEN, D.; JIAJIE, L.; HAILIN, F.; SHENGYONG, C. Image reconstruction of internal defects in wood based on segmented propagation rays of stress waves. Appl. Sci., v.8, n. 1778 p.1-18, 2018.